Wireless Power Transfer circuit for e-bike battery charging system

Marino Coppola
PNP Lab srl
Naples, Italy
marino.coppola@unina.it

Pasquale Cennamo
PNP Lab srl
Naples, Italy
pacocennamo@gmail.com

Adolfo Dannier
Department of Electrical Enginneering and Information Technologies
University of Napoli – Federico II
Napoli, Italy
adannier@unina.it

Diego Iannuzzi
Department of Electrical Enginneering and Information Technologies
University of Napoli – Federico II
Napoli, Italy
iandiego@unina.it

Santolo Meo
Department of Electrical Enginneering and Information Technologies
University of Napoli – Federico II
Napoli, Italy
santolo.meo@unina.it

***Abstract*—In this paper a Serie Series-Resonant Inductive Power Transfer (SS-RIPT) circuit for wireless e-bike battery charger is proposed. The system architecture is accurately described, while highlighting the main features of a suitable design procedure. A simulation model is developed in PSIM software to verify the circuit is fully functional. A full-scale proptotype of a 80 *W* battery charger has been realized, with particular attention to the layout optimization in order to minimize weight and volume of the final product. Moreover, it is equipped with two XBee-Pro S2 radios to also obtain a wi-fi communication between the primary and secondary side. Experimental tests carried out on the prototype confirm the effectiveness of the proposed design and control approach.**

Keywords—wireless power transfer, resonant converter, e-bike battery charger.

I. INTRODUCTION

Wireless Power Transfer (WPT) is a well-known technology which enables, by means of electromagnetic field, a power source to transmit energy to an electrical load across an air gap, without interconnecting cables. The two main methods for WPT are: radiative (i.e., radio frequency (RF) based) and non-radiative (i.e., coupling-based) [1]. The first one is used in very low power application due to the safety issue arising from the exposure to RF waves, while the second method is based on the coupling of magnetic field between two coils, so overcoming the previous issue. It is possible to have a capacitive or inductive coupling WPT. This latter represents the favorite choice for its reduced effect on the human body thanks to the lower intensity of the electric field.

The WPT technology based on inductive coupling is called Inductive Power Transfer (IPT), which has assumed, in the last years, a relevant role in several fields such as biomedics, consumer electronics (e.g. smartphone), clean factory automation and green mobility [2],[3]. It is clear that IPT applications can spread from low-power to medium-high power systems [4]. As a consequence, the research interest is now focused on the improvements in terms of power efficiency and possible transmitting distance [5]. In particular, the use of resonance circuit topology, for both the primary and secondary side of an IPT system, can lead to better performance for larger separation distance and for power transfer capability, if the operating frequency exploits the resonant frequency. This circuit topology is referred as RIPT (Resonant Inductive Power Transfer), which is considered an excellent solution for mid-range wireless powering [5]. It consists of two independent mutually coupled electrical circuits (i.e., primary and secondary side), basically representing a two-coil system, which is a loosely coupled transformer [6]. This latter provides a large leakage flux, so resulting in poor coupling coefficient or rather reduced efficiency. In order to overcome this negative effect, a compensation network is required, thus capacitors can be connected in series or parallel with the coils. Four main circuit topologies based on series and/or parallel LC resonant circuit configuration can be identified: series-series (SS), series-parallel (SP), parallel-series (PS), and parallel- parallel (PP). In all cases, the fundamental requirement for the compensation capacitor is to resonate with the primary and/or the secondary inductance [2], thus properly tuning the system performance. The primary compensation network is useful to minimize the VA rating of the power supply, so improving the power factor, while the secondary compensation network acts to enhance the power transfer capability. Among the four aforementioned circuit topologies, the most used is the series-series because of better performance in terms of efficiency [7]. The SS-RIPT topology represents a double-tuned circuit (i.e., a resonant tank is present on each side of the circuit) operated at the resonant frequency ω_0, which is the zero-phase angle (ZPA) frequency. Nevertheless, in such a circuit, it is possible to have more than one zero-phase angle (ZPA) frequency or rather multiple resonant frequencies exist. This phenomenon is known as bifurcation [8], and can be observed when the coupling coefficient k is greater than a critical value, k_c. In order to guarantee stable circuit operation the bifurcation should be avoided, so particular care should be taken to properly design the magnetic components.

Nowadays, the most promising use of RIPT circuit is the contactless battery charging, which falls into the so-called near-field applications. In this paper, a RIPT circuit for e-bike charging station is proposed to favor the use of a bike sharing service in order to enhance the green inter-mobility in urban context. The main advantages are related to the absence of a plug-in, so resulting more user-friendly than traditional system, while also assuring a higher safety due to the galvanic insulation between the primary (e.g., the charging station) and the secondary circuit (e.g., e-bike). This latter feature also ensure a greater reliability, ease of maintenance and longer product life-time. Moreover, the galvanic insulation and the corresponding absence of electrical cables and mechanical contacts allows the system

978-1-5386-4192-7/18/$31.00 ©2018 IEEE

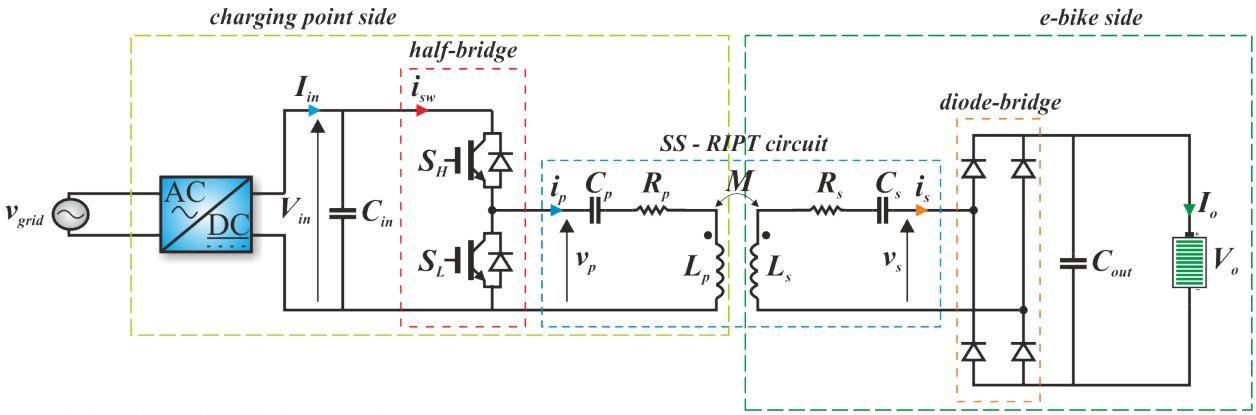

Fig. 1. Wireless charger for e-bike battery pack.

to be operated in ultraclean as well as ultradirty environment [9], so accomplishing with the requirements of an out-door service. This paper is particularly devoted to the e-bike charger design in terms of architecture and hardware implementation in order to provide a final product of reduced weight and dimensions, which could be easily adapted to traditional e-bike and e-bike station as retrofit system. In addition to the WPT, the proposed design also provides a wireless communication system consisting of two XBee-Pro S2 radios based on the ZigBee protocol, useful to transmit measured data from the secondary to the primary side for control purpose.

The paper is organized as follows. System description and principle of operation are presented in Section II. The numerical results performed in PSim environment are reported in Section III. The hardware implementation and the experimental results on a full-scale test-rig are provided in Sections IV to demonstrate the effectiveness of the proposed design and control approach. Finally, conclusions are drawn in Section V.

II. System Description

The architecture of the SS-RIPT circuit is shown in Fig. 1. The main power source is the utility grid (i.e., 230 V_{rms}, 50 Hz), then a AC-DC converter provides the input DC voltage V_{in}. The half-bridge stage converts the obtained DC voltage into the high-frequency AC voltage v_p. As a consequence, the high-frequency AC power resonates in the primary compensation tank and primary coil with a resonant frequency f_0 tuned to the switching frequency at which the power semiconductor devices are operated [6]. The high-frequency AC power flows in the primary loop coil, so generating a magnetic field around it, which is induced at the secondary loop coil. The induced high-frequency AC voltage, v_s, is, then, converted to DC voltage by means of a diode-bridge rectifier with a capacitive filter, C_{out}. The output DC voltage V_o is applied to the battery pack.

In such a circuit, the coupling between primary and secondary side is weak, thus resulting in reduced power transfer. In order to overcome this issue a proper compensation of the leakage inductance should be adopted by using capacitive tank.

The primary compensation network is useful to reduce the needed source VA rating with the aim of obtaining unity power factor. In fact, the inherent reactive nature of the impedance seen by the source itself affects the power factor [10]. In addition, reactive power circulation produces resistive losses, so reducing system efficiency.

The secondary compensation circuit is useful to improve the power transfer capability. The maximum is reached when the secondary is tuned to the resonant frequency, so the choice of the secondary compensation capacitance is made to allow resonance.

The main advantages of the SS-RIPT circuit topology are well-known [8], [11]: the primary capacitance C_p is independent of mutual inductance M and of load and the reflected reactance is zero.

The suitable design procedure is reported in [12]: the main objective was to determine the values of electrical and electromagnetic circuit parameters, for a SS-RIPT configuration, in order to accomplish with the previous requirements in terms of power transfer capability, while also avoiding the bifurcation phenomenon. The obtained values are reported in Table I.

Table I. Circuit parameters of the e-bike charger.

Symbol	Description	Value
L_p, L_s	Primary, secondary self-inductance	91.3 μH
R_p, R_s	Equivalent primary, secondary resistance	61.8 $m\Omega$
M	Mutual inductance	30 μH
C_p, C_s	Primary, secondary compensation capacitance	180 nF
f_0	Resonant frequency	40 kHz
V_{in}	Rated input DC voltage	48 V
V_o	Rated output DC voltage	42 V
P_o	Rated output power	80 W
R_o	Rated output resistance	22 Ω

The designed magnetic pads are in EE cores geometry configuration, which is preferred solution w.r.t. SS cores because of improved mutual coupling and lesser leakage flux [12]. The core material is a ferrite material with a relative permeability of 2300 with a flux density saturation level of 0.42 T. The capacitance value of input capacitor C_{in}=4·330 μF=1.32 mF is due to the possibility of power source to provide the needed current, while maintaining a stable dc-link input voltage level. The capacitance value of output filter capacitor is C_{out}=3·680 μF≈2 mF to guarantee a stable output voltage. Moreover, the sizing of C_{out} is related to the system dynamics, which is dictated by the output RC circuit. As a consequence, the time constant τ=R_oC_{out} poses a

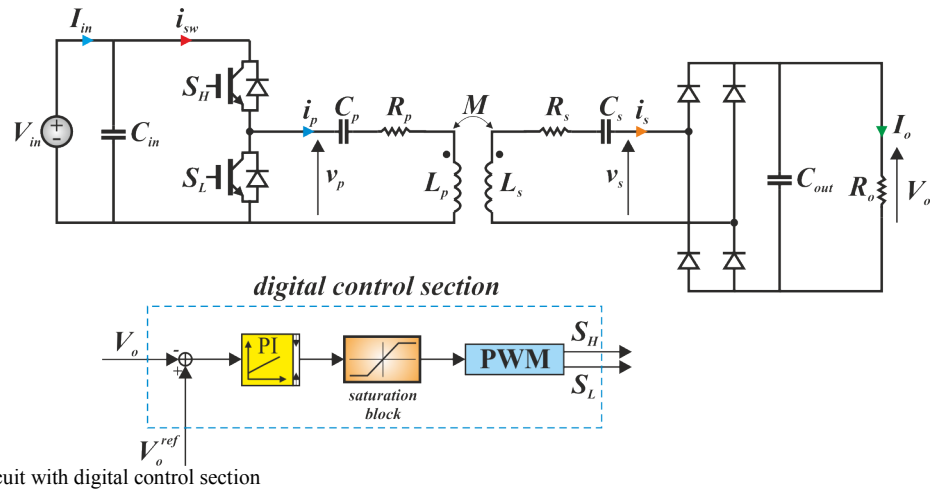

Fig. 2. Simulated circuit with digital control section

constraint on the system time response. In addition, it must be taken into account the time interval needed for proper wi-fi communication between primary and secondary side by means of ZigBee protocol or rather the digital controller acts only every time that new data are received, so it has been designed to ensure adequate dynamic behavior.

III. Simulated Performance

The electrical scheme shown in Fig. 1 has been simplified by directly considering a voltage DC source equal to V_{in}, so implementing the main DC/DC conversion stage (see Fig. 2). Moreover, the battery pack is replaced by a resistive load R_o=22 Ω. This latter value is due to the ratio between the square value of desired output voltage V_o and the maximum power of the battery, P_o.

$$R_o = V_o^2 / P_o = (42)^2 / 80 \simeq 22\,\Omega \qquad (1)$$

The battery pack, provided with the used e-bike, has a maximum power of P_o=80 W and only requires, as input, a DC voltage of 42 V. In fact, the battery is equipped with an internal DC/DC converter, which is able to properly regulate the charging process. As a consequence, the main control purpose is to stably provide the suitable voltage at the battery terminals. To reach the desired behavior a voltage error control is used. At this aim a simple linear digital PI controller is implemented without additional processing, so resulting in faster and accurate response [7]. Besides, it is not necessary a current sensor as in other control techniques (e.g., power control, etc…), thus reducing cost and volume of the final circuit.

The control scheme is shown in Fig. 2, while the used circuit parameters values are the same reported in Table I. The measured battery voltage is subtracted from the desired reference voltage, thus obtaining the voltage error, which is properly sampled to become the input of a digital PI controller. Then, a saturation block is able to maintain the duty cycle in the desired range (0; 0.5]. Finally, the PWM (Pulse Width Modulation) block generates the gate signals for the half-bridge converter. The operating frequency is fixed at the resonance frequency (i.e., 40 kHz) in order to maximize the power transfer capability. The used control method falls under the fixed frequency strategies, which are better suited for application where no dynamic variation of circuit parameters occurs as in the case of static charging system based on SS-RIPT architecture.

Fig. 3 shows the steady-state behavior of the main circuit voltages and currents, obtained by means of PSim simulator. The Fig. 3.a) reports the primary and secondary current waveforms, which both result almost sinusoidal. The primary and secondary voltages are shown in Fig. 3.b) and, as expected, they result in high-frequency (i.e., resonance frequency) square-waves. In particular, the primary voltage is a positive quantity spanning from zero to V_{in} as per the connection of the half-bridge. Fig. 3.c) highlights the stable behavior of the output voltage, which reaches the desired voltage level of 42 V. The overall efficiency of the DC/DC converter with SS-RIPT link is of about 87%.

IV. Experimental Set-up

A full-scale prototype of the resonant DC/DC converter circuit was built in order to prove the validity of the proposed design and control approach. Fig. 4 shows a picture of the realized circuit. Each of the two switching devices of the half-bridge was replaced by a powerMOS (Infineon IPB64N25S3-20 with a break-down voltage of 250 V and a continuous drain current of 46 A at T=100°C) with an

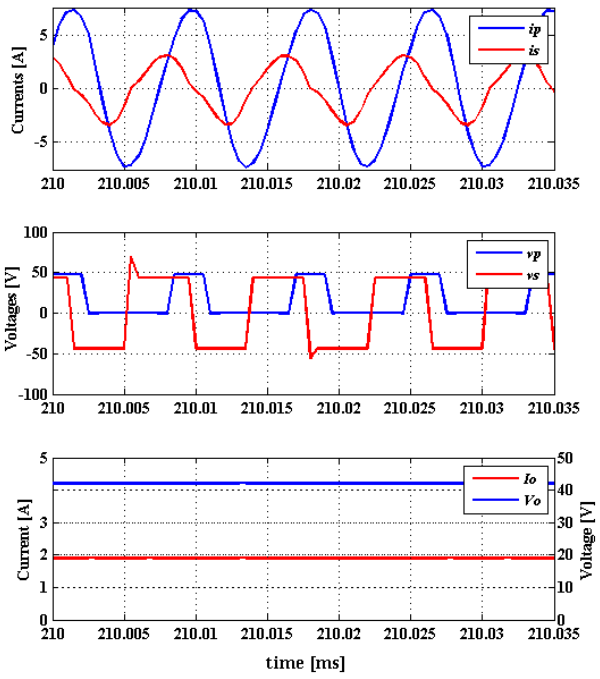

Fig. 3. Simulated performance: a) primary and secondary currents; b) primary and secondary voltages; c) load voltage and current.

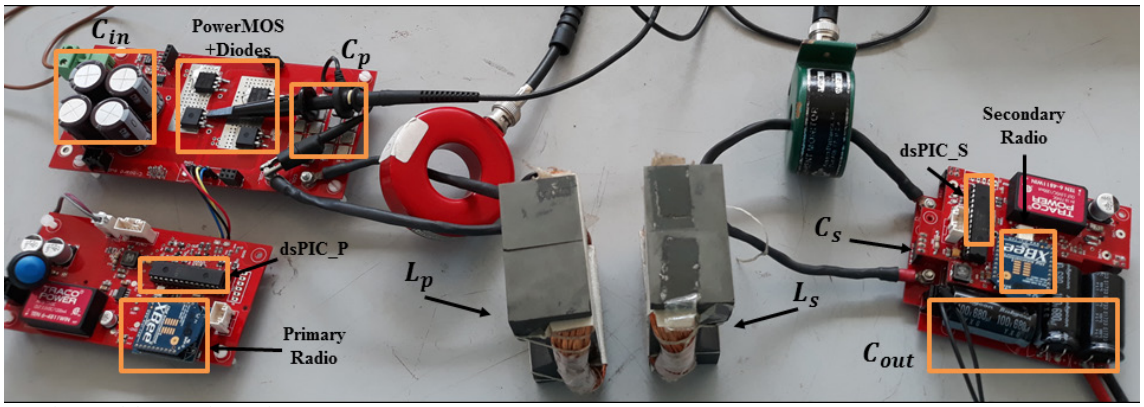

Fig. 4. Picture of the experimental set-up.

anti-parallel Schottky diode. The diode bridge rectifier was composed of four fast recovery power diodes (STMicroelectronics STTH30L06G-TR) with a reverse voltage of 600 V and a forward current of 30 A.

The primary compensation capacitance as well as the secondary one was obtained by the parallel connection of 18 multilayer ceramic capacitors of 10 nF each (Kemet C2225C103JCGACTU), so also reducing the total ESR (Equivalent Series Resistance). The dc-link input capacitance was realized by means of parallel connection of four electrolytic capacitors of 330 μF (Nichicon UCS2D331MHD), while the output capacitance was obtained with the parallel connection of three electrolytic capacitors of 680 μF (Nichicon UHE2A681MHD). The high-frequency transformer was custom designed and its main features were described in [12].

The control algorithm was implemented on a Microchip dspic33FJ16GS502, while the communication between the primary (i.e., charging station) and secondary (i.e., e-bike) side was obtained by means of two XBee-Pro S2 radios based on the ZigBee protocol. For control purpose it is necessary only to measure the battery voltage, whose value is reported to the primary side, where the main controller is located, thanks to wi-fi communication.

Great attention was devoted to the layout design with the aim of minimizing the circuit dimensions, in particular for the secondary side, which represents the on-board e-bike circuit. The dimensions are:

- Primary board (WxLxH): 7.5x15x3 *cm*
- Secondary board: (WxLxH): 7.8x9x2 *cm*

Moreover, the realized circuit can be easily adapted to different charging stations, thus resulting in a flexible retro-fit product.

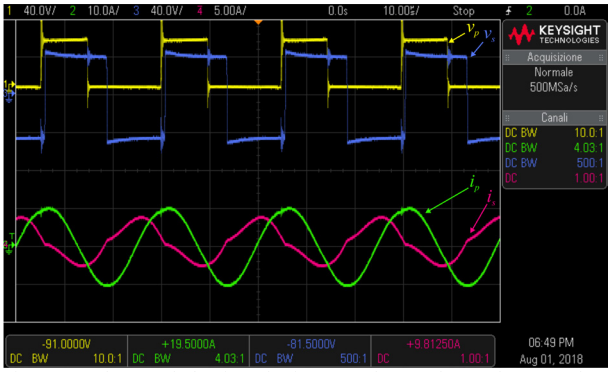

Fig. 5. Steady-state behavior of primary and secondary voltages and currents.

A. Experimental test

In order to perform the test and proper measurements, the circuit was decomposed as in Fig. 4.

The blue push button emulates the e-bike presence at the charging station, thus pushing the button kick-off the charging procedure. This latter is divided in the following main steps:

- Initially, a predefined control starts with a default value of the duty cycle equal to 0.2.
- The primary radio (i.e., the master) starts to send message to the secondary radio (i.e., the slave). When the secondary responds, it means that the secondary circuit is properly supplied by the primary. This procedure has a time duration of 3 s.
- If the previous step is successfully completed, the secondary radio sends to the primary the first voltage measure, thus the actual control can now start.

Moreover, it is worth noting that a current sensor is added in order to monitor the current i_{sw} (see also Fig. 2). If the measured current overcomes the fixed upper or lower limit, a safety procedure starts to switch off the power devices, while interrupting the control.

The steady-state behavior of primary and secondary voltages and currents is reported in Fig. 5. It can be noted that the currents are almost sinusoidal and in good agreement with the simulated performance as well as the voltages waveforms. The steady-state value of the battery voltage, is stably equal to the reference voltage of 42 V. The overall efficiency reached during the experiment was equal to 81%.

V. Conclusions

This paper has been focused on the design and control of an e-bike battery charger based on a wireless power transfer circuit topology. In particular, a SS-RIPT circuit for e-bike charging station is proposed to favor the use of a bike sharing service also thank to a more user-friendly system than traditional ones. A proper system description has been provided in order to highlight the main features of the chosen circuit architecture, so determining the suitable design procedure. A numerical analysis has been conducted to show the correctness of the aforementioned design procedure, while also testing the control strategy. A full-scale prototype

of a 80 W e-bike battery charger has been built and the experimental results clearly show the effectiveness of the proposed design and control approach.

REFERENCES

[1] X. Lu, P. Wang, D. Niyato, D. I. Kim and Z. Han, "Wireless Charging Technologies: Fundamentals, Standards, and Network Applications," in *IEEE Communications Surveys & Tutorials*, vol. 18, no. 2, pp. 1413-1452, Secondquarter 2016.

[2] W. Zhang and C. C. Mi, "Compensation Topologies of High-Power Wireless Power Transfer Systems," in *IEEE Transactions on Vehicular Technology*, vol. 65, no. 6, pp. 4768-4778, June 2016.

[3] G. A. Covic and J. T. Boys, "Modern Trends in Inductive Power Transfer for Transportation Applications," in *IEEE Journal of Emerging and Selected Topics in Power Electronics*, vol. 1, no. 1, pp. 28-41, March 2013.

[4] B. X. Nguyen *et al*., "An Efficiency Optimization Scheme for Bidirectional Inductive Power Transfer Systems," in *IEEE Transactions on Power Electronics*, vol. 30, no. 11, pp. 6310-6319, Nov. 2015.

[5] J. Kim, G. Wei, M. Kim, J. Jong and C. Zhu, "A Comprehensive Study on Composite Resonant Circuit-Based Wireless Power Transfer Systems," in *IEEE Transactions on Industrial Electronics*, vol. 65, no. 6, pp. 4670-4680, June 2018.

[6] Zicheng Bi, Tianze Kan, Chunting Chris Mi, Yiming Zhang, Zhengming Zhao, Gregory A. Keoleian, A review of wireless power transfer for electric vehicles: Prospects to enhance sustainable mobility, Applied Energy, Volume 179, 2016, Pages 413-425.

[7] Z. Huang, S. Wong and C. K. Tse, "Control Design for Optimizing Efficiency in Inductive Power Transfer Systems," in *IEEE Transactions on Power Electronics*, vol. 33, no. 5, pp. 4523-4534, May 2018.

[8] K. Aditya and S. S. Williamson, "Design Guidelines to Avoid Bifurcation in a Series-Series Compensated Inductive Power Transfer System," in *IEEE Transactions on Industrial Electronics*. doi: 10.1109/TIE.2018.2851953.

[9] W. Zhang, S. Wong, C. K. Tse and Q. Chen, "Design for Efficiency Optimization and Voltage Controllability of Series–Series Compensated Inductive Power Transfer Systems," in *IEEE Transactions on Power Electronics*, vol. 29, no. 1, pp. 191-200, Jan. 2014.

[10] K. Aditya and S. S. Williamson, "Comparative study of Series-Series and Series-Parallel compensation topologies for electric vehicle charging," *2014 IEEE 23rd International Symposium on Industrial Electronics (ISIE)*, Istanbul, 2014, pp. 426-430.

[11] Chwei-Sen Wang, G. A. Covic and O. H. Stielau, "Power transfer capability and bifurcation phenomena of loosely coupled inductive power transfer systems," in *IEEE Transactions on Industrial Electronics*, vol. 51, no. 1, pp. 148-157, Feb. 2004.

[12] Diego Iannuzzi, Luigi Rubino, Luigi Pio Di Noia, Guido Rubino, Pompeo Marino, Resonant inductive power transfer for an E-bike charging station, Electric Power Systems Research, Volume 140, 2016, Pages 631-642.